
PERGAMON

Journal of Quantitative Spectroscopy & Radiative Transfer 68 (2001) 657–677

Journal of Quantitative Spectroscopy & Radiative Transfer

www.elsevier.com/locate/jqsrt

Zenith-sky observations of stratospheric gases: the sensitivity of air mass factors to geophysical parameters and the influence of tropospheric clouds

Matthew R. Bassford[a], Chris A. McLinden[b], Kimberly Strong[a,*]

[a]*Department of Physics, University of Toronto, 60 St. George Street, Toronto, ON, Canada M5S 1A7*
[b]*Department of Earth System Science, University of California at Irvine, Irvine, CA 92697-3100, USA*

Received 10 November 1999; accepted 19 May 2000

Abstract

The retrieval of accurate vertical column amounts of stratospheric constituents from zenith-sky spectroscopy is dependent on accurately modeling the transfer of radiation through the atmosphere and calculating suitable air mass factors (AMFs). Using a vector radiative transfer (RT) model we evaluate potential error sources in the AMF calculation, arising from incorrect geophysical parameters and computational approximations. Ozone and NO_2 AMFs were calculated using 19 different parameterizations, whereupon each was used to retrieve vertical column information from zenith-sky spectra recorded at a mid-latitude location. When the model was run with single-order scattering only, the derived AMFs were between 2 and 5% lower than those calculated using a multiple scattering scheme. Multiple scattering was also found to act in tandem with other parameters investigated, for example volcanic sulfate aerosols and surface albedo, and as such, we conclude that it is important to include multiple scattering in any RT model. Significant errors were also introduced by using a standard ozone profile rather than one derived from ozonesonde data. Substantially amplified AMFs were obtained from model runs that contained tropospheric clouds. Zenith-sky measurements recorded during cloudy conditions demonstrated that AMFs calculated from an RT model that neglects scattering by tropospheric clouds are unsuitable for analysis of spectra from overcast days. The feasibility of calculating AMFs tailored to account for the presence of clouds is also discussed.

Keywords: Radiative transfer model; Zenith-sky spectroscopy; Air mass factor (AMF); Cloud; Ozone; NO_2

* Corresponding author. Fax: + 1-416-978-8905.
E-mail addresses: matt@atmosp.physics.utoronto.ca (M.R. Bassford), strong@atmosp.physics.utoronto.ca (K. Strong).

0022-4073/01/$ - see front matter
PII: S0022-4073(00)00052-2

1. Introduction

The measurement of trace stratospheric constituents such as ozone and nitrogen dioxide (NO_2) by means of differential optical absorption spectroscopy (DOAS) is a well-established and widely employed technique (e.g. [1–4]). Traditionally, ground-based measurements employing a zenith-sky viewing geometry have been made, but more recently DOAS has been successfully applied to nadir-viewing instruments on aircraft [5] and satellite [6] platforms. Ground-based zenith-sky observations are made at numerous sites around the world to furnish information about ozone trends and the processes that influence its abundance. Measurements at key sites are performed as part of the Network for the Detection of Stratospheric Change (NDSC), which coordinates and collates observations. In addition to the quality of the measured spectral data, the accuracy of ozone and NO_2 vertical columns derived from zenith-sky measurements is dependent on how well the transfer of radiation through the atmosphere can be modeled. While interpreting direct solar measurements is relatively straightforward (because the light travels along a single optical path), the analysis of zenith-sky observations necessitates a more complex treatment. Instruments employing zenith-sky-viewing geometry receive sunlight scattered from a range of altitudes along a random-walk path. Furthermore, because the intensity measured at the ground varies exponentially with optical depth, the total slant column is not equal to the sum of effective slant columns for different scattering altitudes.

Comprehensive reviews of zenith-sky DOAS have been presented elsewhere [7,8] but a brief synopsis of the technique is given here. Scattered sunlight observed at twilight traverses a much longer stratospheric path than scattered sunlight observed at noon. As a result, the apparent slant column density of any species having a maximum concentration in the stratosphere (e.g. ozone and NO_2) is much greater in twilight spectra than noon spectra. For example, the calculated ozone optical depth (at 510 nm) is typically 16–17 times greater at a solar zenith angle (SZA) of 90° than if the sun was directly overhead (SZA = 0°) [9]. Vertical column amounts of stratospheric species can be deduced by comparing the observed slant column densities with an appropriate enhancement factor, referred to as the air mass factor (AMF). AMFs are calculated using a radiative transfer (RT) model. A recent comparison between four different RT models [10] reported a relatively good inter-model agreement (6%) when NO_2 AMFs were calculated at a SZA of 90°. In addition to differences between model schemes, accurate AMFs calculations require a rigorously modeled atmosphere constrained by realistic geophysical parameters, including vertical profiles of absorber number density, aerosol abundance and temperature. This is to ensure that scattering events and absorption of radiation in the real atmosphere are replicated in the model. Standard values (e.g. [11,12]) are often used, although actual values will obviously differ from the assumed climatology.

Historically, the influence of clouds on zenith-sky measurements has been largely neglected, because the geometry of zenith-sky observations dictates that stratospheric pathlengths far exceed tropospheric paths at twilight. Furthermore, for measurements of ozone and NO_2 taken a suitable distance (at least 200 km) away from urbanized areas, there is little advection of tropospheric pollution to the observation site and the bulk of the absorbing column is located in the stratosphere. However, in recent years increasing attention has been paid to errors in retrieved column amounts that can be introduced by the presence of tropospheric clouds [13–15]. Additional tropospheric pathlengths of over 100 km have been inferred for spectral observations taken under

cloudy skies [13,16] with the implication that the caliber of zenith-sky measurements can be severely compromised.

The main focus of this paper is to examine AMFs calculated using an RT model and systematically investigate how they vary with changes in the model atmosphere. We present results from a sensitivity study and evaluate which geophysical parameters in the RT model are most likely to adversely affect the derived AMFs. AMFs calculated using climatological values are compared with observed data. The AMFs are used to retrieve vertical column densities of ozone and NO_2 from zenith-sky measurements recorded using a UV–visible grating spectrometer at a mid-latitude site. Our conclusions are then compared with the results of previous evaluations [9,17] and the implications for zenith-sky measurements are discussed. AMFs are also calculated for atmospheres containing tropospheric clouds in an attempt to predict the effect on zenith-sky observations and account for the enhanced optical depths that were observed during cloudy conditions.

2. Methods

2.1. Zenith-sky measurements

Ground-based zenith-sky measurements were recorded using a UV–visible grating spectrometer during August 1998. The measurements were part of the Middle Atmosphere Nitrogen TRend Assessment (MANTRA) field campaign that took place in Vanscoy, SK, Canada (52° 01′N, 107° 02′W, elevation 511 m). The MANTRA campaign was centered on a suite of measurements made during a high-altitude balloon flight (August 24, 1998) designed to investigate the odd-nitrogen budget of the stratosphere [18]. Balloon-borne measurements were complemented by ground-based observations and regular ozone- and radio-sonde launches during the two weeks prior to launch. The campaign thus provided an excellent opportunity to make ground-based measurements of a relatively well-characterized atmosphere and obtain accurate parameters for input into the RT model.

The ground-based spectrometer and measurements from the MANTRA campaign are described more fully in a separate publication [19], however brief details of the instrument and operating procedure follow. The spectrometer used to acquire the measurements (Triax 180, JY Horiba, Edison NJ) was fitted with an adjustable entrance slit and a triple grating turret to ensure flexibility in spectral range and resolution. The data presented here was acquired with a slit width of 50 μm and a diffraction grating ruled at 600 grooves/mm, which produced a full-width half-maximum (FWHM) resolution of 0.90 nm. The detector was a CCD array (2000×800 pixels, each 15 μm × 15 μm), thermoelectrically cooled to $-30°C$, with a sampling ratio (8.5 pixels/FWHM) sufficient to minimize aliasing artifacts [20].

Zenith-sky spectra (320–554 nm) were recorded during each twilight period (SZAs between 80 and 96°) of the field campaign. A set of noon reference spectra was also acquired at high sun, when the SZA was typically 40°. The results presented here are from analyses using a common reference spectrum recorded on Julian-Day 237 (J-237) (August 25), 1998. Most recent publications that present ozone and NO_2 measurements also use a common reference, rather than a daily reference spectrum (e.g. [21,22]). The benefits of this approach are twofold: firstly, all differential optical

depths are relative to the same spectrum and secondly, a reference spectrum recorded on a clear day can be selected.

2.2. Retrieving vertical column information from zenith-sky spectra

Zenith-sky spectra recorded with the ground-based spectrometer were analyzed using a DOAS retrieval procedure based on that of Fish et al. [3] to determine ozone and NO_2 column amounts using spectral regions between 450–540 and 410–455 nm, respectively. Cross sections of ozone [23], NO_2 [24], H_2O [25], and O_4 [26] respectively] were fitted to the differential spectra using a simultaneous non-linear least-squares routine. A correction for the Ring effect was made using a modeled Ring 'cross-section' [27]. From the fitted optical depth of each absorber, the differential slant column density (SCD) was retrieved. Absorption by BrO and OClO over the wavelengths of interest was assumed to be negligible for the mid-latitude summer atmosphere.

The vertical column density at SZA θ, VCD(θ), is related to SCD(θ) as shown in Eq. (1), which can be rearranged to resemble the form $y = mx + c$ (Eq. (2)):

$$\mathrm{VCD}(\theta) = \frac{\mathrm{SCD}(\theta) + \mathrm{RCD}}{\mathrm{AMF}(\theta)}, \tag{1}$$

$$\mathrm{SCD}(\theta) = \mathrm{VCD}(\theta) \times \mathrm{AMF}(\theta) - \mathrm{RCD}. \tag{2}$$

In Eqs. (1) and (2), RCD is the amount of absorber in the reference spectrum and AMF(θ) is the air mass factor at SZA θ. If the observed ozone slant columns for a set of twilight spectra are plotted against the corresponding AMFs (the so-called Langley plot), then the slope of the line is equal to VCD(θ). The y-intercept should be equal to negative RCD although it can also contain instrumental artifacts [28]. The Langley plot for sunrise on August 20, 1998 (J-232) is shown as Fig. 1. In general, VCDs for ozone are either derived from the slope of the Langley plot (yielding one value per twilight set), or the previously derived value of RCD is substituted into Eq. (1) and all SCDs are converted into VCDs [29].

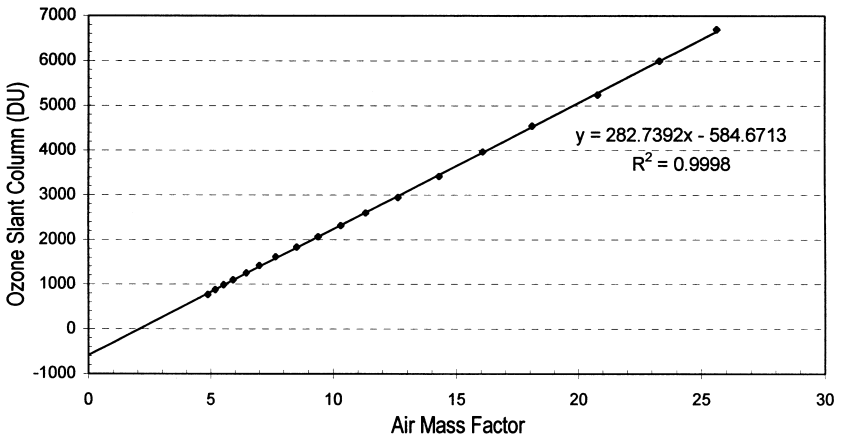

Fig. 1. Langley plot of SCD vs. AMF for sunrise on August 20, 1998 (J-232).

While Langley plots provide an elegant method for deriving ozone column information, they are poorly suited for the analysis of NO_2 due to diurnal changes in the chemical partitioning between NO_2 and N_2O_5. The NO_2 vertical column increases throughout the day, as N_2O_5 is photolyzed to NO_2. Consequently, NO_2 VCDs are calculated from Eq. (1) with a value of RCD chosen to produce a smoothly increasing column amount through the day [29]. Alternatively, a photochemical model can be used to predict the value of RCD(θ) [30].

2.3. Radiative transfer model

AMFs for the zenith-sky measurements were calculated using the model of McLinden et al. [31,32], which solves the RT equation using successive orders of scattering in an inhomogeneous atmosphere. An iterative calculation of radiance for photons scattered once, twice, three times (etc.) was performed with the total radiance taken as the sum over all scattering orders (e.g. [33]). The direct solar beam and all scattering orders were calculated in a spherical atmosphere. At present, refraction is not included in the model, but this is believed to have only a small effect on AMFs for stratospheric absorbers [17]. This model has recently been employed in the retrieval of BrO from spectroscopic measurements made onboard the high-altitude ER-2 aircraft [5].

Necessary geophysical inputs into the RT model included vertical profiles of air number density, temperature, absorber number densities, and aerosol number density. Other inputs required were aerosol size distributions, refractive indices and surface albedo. Absorption by O_4 was also included in the model. A 5% perturbation applied to the entire profile was used to calculate AMFs for ozone (at 505 nm), NO_2 (at 430 nm) and O_4 (at 477 nm) from the following equation:

$$\mathrm{AMF} = -\frac{\ln(I/I_0)}{\sigma \times \Delta\mathrm{column}}. \tag{3}$$

Here, I_0 is the incident radiance on the instrument for a given atmosphere and I is the radiance for the same atmosphere after perturbing the absorber profile. σ is the absorption cross section and Δcolumn the change in absorber column density. The wavelength corresponding to the center of each spectral fitting window was used for AMF calculations as the central wavelength has been shown to be optimal for DOAS retrievals in the visible region [6]. AMFs were tabulated as a function of SZA in 0.1° increments and AMF(θ) for any given twilight spectrum was determined through linear interpolation. Interpolation, as opposed to direct calculation at specified SZAs, was found to have a negligible impact on AMF values.

This model has previously been compared with other vector RT models [34,35] for a variety of plane-parallel, homogeneous atmospheres consisting entirely of either Rayleigh or Mie scattering events. The overall agreement between AMFs calculated from the models was excellent, with maximum errors less than 0.5% for a simulation of the thick (optical depth = 10) Venusian atmosphere and less than 0.1% for optical depths not exceeding unity. In addition, tests of the model in scalar-spherical mode have been carried out against other models: a doubling and adding (D&A) one-dimensional model (E. Griffioen, personal communication, 1999) and a three-dimensional spherical backward Monte-Carlo (BMC) model (L. Oikarinen, personal communication, 1999). Agreement was good with the D&A model (average difference of 0.5% without aerosols and 1.1% with volcanic aerosols) and reasonable with the BMC model ($<4\%$ without aerosols).

3. Radiative transfer model sensitivity study

3.1. AMF calculations using different parameters

The purpose of this study was to compare ozone and NO_2 AMFs for zenith-sky measurements made during MANTRA 1998, calculated under different geophysical and computational regimes. Initially, the RT model was parameterized using all available observed geophysical data, with a rigorous treatment of radiative transfer that included multiple scattering. AMFs derived from these calculations were considered to be a very good estimate of the true mid-latitude atmosphere and are summarized in Table 1. The parameters used in the model were as follows.

Vertical profiles for air number density, temperature and ozone were generated by averaging data from three sonde flights (11, 18 and 23 August 1998) remapped onto a 0.5 km vertical grid [19]. A standard mid-latitude NO_2 profile was assumed (J. Stegman, personal communication) and a background stratospheric sulfate extinction coefficient profile (at 525 nm) was taken from the SAGE II database [36]. The sulfate profile used was from August 1997 (no 1998 data were available at the time of writing) at 50°N and is shown in Fig. 2. The Earth's surface was considered to be Lambertian with an albedo of 0.2, a typical value for summertime grassland [37]. Absorption cross sections for ozone and NO_2 [23,24] were varied as a function of altitude to account for changing temperature. Cross sections at 221, 241 and 273 K were used, with quadratic interpolation employed to determine the cross sections at other temperatures. Similarly, the O_4 cross section [26] was varied with altitude to reflect its pressure dependence. The maximum height of the model atmosphere was 120 km (mapped onto a 0.5 km grid). Note that default AMFs were calculated in scalar mode as including polarization in the RT model increased the run time by a factor of four. Polarization was expected to exert a minor influence on AMFs, and later model runs confirmed this.

Following AMF calculations under the default conditions, each parameter was varied in turn in order to investigate its weighting on the calculated ozone and NO_2 AMFs. Parameters substituted into the model were selected on the basis that they were either standard mid-latitude profiles, approximations that have been used in other model schemes or plausible aerosol climatologies for

Table 1
Default air mass factors for ozone and NO_2 at a range of SZAs

Solar zenith angle	Ozone AMF (505 nm)	NO_2 AMF (430 nm)
40.0	1.388	1.507
60.0	2.019	2.223
80.0	4.851	5.511
82.0	5.730	6.525
84.0	6.979	7.965
86.0	8.825	10.104
88.0	11.629	13.450
90.0	15.900	18.919
92.0	21.977	27.048
94.0	26.673	33.117

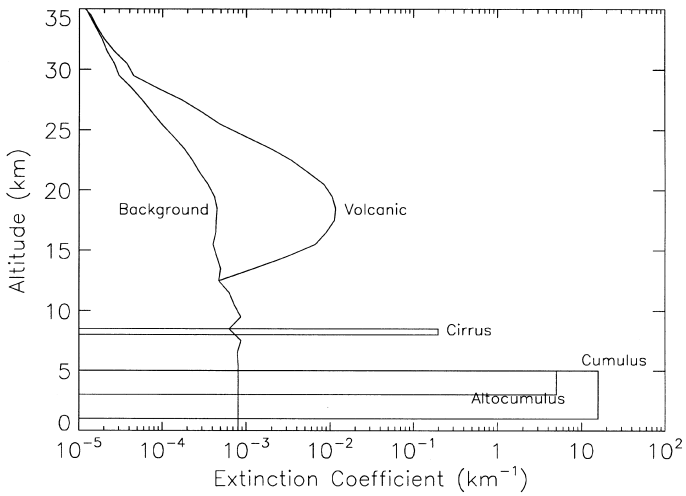

Fig. 2. Vertical profiles of aerosol extinction coefficients.

Table 2
Summary of different aerosol types used in air mass factor calculations

Aerosol type	Size distribution[a] (a, b)	Composition[b]	Effective radius (μm)	Optical depth at 525 nm	Number density (cm^{-3}) at Max. Conc.
Background stratospheric sulfates	Log-normal (0.11, 0.44)	75% H_2SO_4 25% H_2O	0.18	0.015	10.7
Volcanic stratospheric sulfates	Log-normal (0.15, 0.44)	75% H_2SO_4 25% H_2O	0.25	0.086	49.5
Cirrus cloud	Standard-gamma (50.0, 0.25)	Ice	50.0	0.1	0.035
Altocumulus	Standard-gamma (8.0, 0.25)	Water	8.0	10.0	26.0
Cumulus	Standard-gamma (8.0, 0.25)	Water	8.0	70.0	101.0

[a]The size distribution parameter pair (a, b) gives the characteristic radius, a, in μm and the dimensionless width, b (see [33]).
[b]Composition only affects the refractive index.

a mid-latitude atmosphere. A variety of different aerosol types were used, as listed in Table 2. A sulfate profile representative of a post-volcanic atmosphere was derived from SAGE II measurements (50°N, September 1992) [36] about 15 months after the eruption of Mt. Pinatubo. From Table 2, it can be seen that the optical depth of the post-volcanic sulfates (0.086) was larger than background aerosol optical depth (0.015) by a factor of six. The remaining aerosols represent three typical tropospheric clouds: thin cirrus near the tropopause (optical depth 0.1, altitude 8 km),

mid-tropospheric altocumulus of moderate optical depth (optical depth 10, altitude 3–5 km), and a thick cumulus layer near the surface (optical depth 70, altitude 1–5 km). The aerosol extinction coefficient profiles are shown in Fig. 2. All aerosol types were assumed to be non-absorbing and spherical, which allowed Mie theory to be used. Log-normal and standard-gamma aerosol size distributions were used to model the different aerosol types, where each was characterized with a radius and distribution width [33].

3.2. Discussion

The RT model sensitivity study was performed to determine which parameters exert the strongest weighting on the AMF calculations and to diagnose potential sources of error in the retrieved VCDs of ozone and NO_2. The effect of model parameterization and assumed number density profiles on ozone and NO_2 AMFs can be seen in Figs. 3 and 4, respectively, and it is apparent that some parameters are more influential than others. Relative percentage differences in the AMFs for each variable changed were calculated using the following equation:

$$\Delta\mathrm{AMF}(\%) = \frac{100(\mathrm{AMF}_{\mathrm{new}} - \mathrm{AMF}_{\mathrm{default}})}{\mathrm{AMF}_{\mathrm{default}}}. \tag{4}$$

To contribute a large error to the retrieved VCD, the error in AMF must be significant relative to the measurement error. To place our results in context, a recent intercomparison exercise between NDSC instruments [21] identified mean fractional differences in SCDs that were within $\pm 2.5\%$ for ozone and $\pm 7\%$ for NO_2. It follows that in general, uncertainties in AMFs due to incorrect parameterization of the RT model present more of an issue with ozone measurements than NO_2. The parameters varied in the current study can be grouped into four loosely defined sets: (a) standard geophysical parameters, (b) RT model approximations, (c) sulfate aerosols and (d) tropospheric clouds. Each is discussed in turn below.

3.2.1. Standard geophysical parameters

A significant error in ozone AMFs (2–5% for most SZAs) was observed when the US standard mid-latitude ozone profile [11] was used. Using a climatological ozone profile for August, 45°N, based on multi-year sonde and satellite measurements [38], these differences were reduced to 1–3%. The different ozone profiles used in AMF calculations are plotted in Fig. 5. The logical conclusion is that sonde measurements should be used when calculating ozone AMFs, but such a priori information is not always available. In these cases we advocate the use of climatological values, which appear to provide a better approximation than the more commonly used US standard profile. However, in a dynamically changing atmosphere (e.g. episodic ozone depletion during polar spring) the use of a climatological ozone profile may also introduce large errors into retrieved column amounts. Sonde data should be used for such measurements.

Atmospheric temperature plays a minimal role in altering AMFs for optically thin absorbers such as the Chappuis ozone bands and NO_2 in the UV–visible region. What determines AMFs is the geometric photon path applied to the shape of the absorption cross-section profile (equal to number density × cross section). As long as absorption is in a linear regime, changes in temperature exert little influence on the shape of the absorption profile. Even when an isothermal atmosphere of

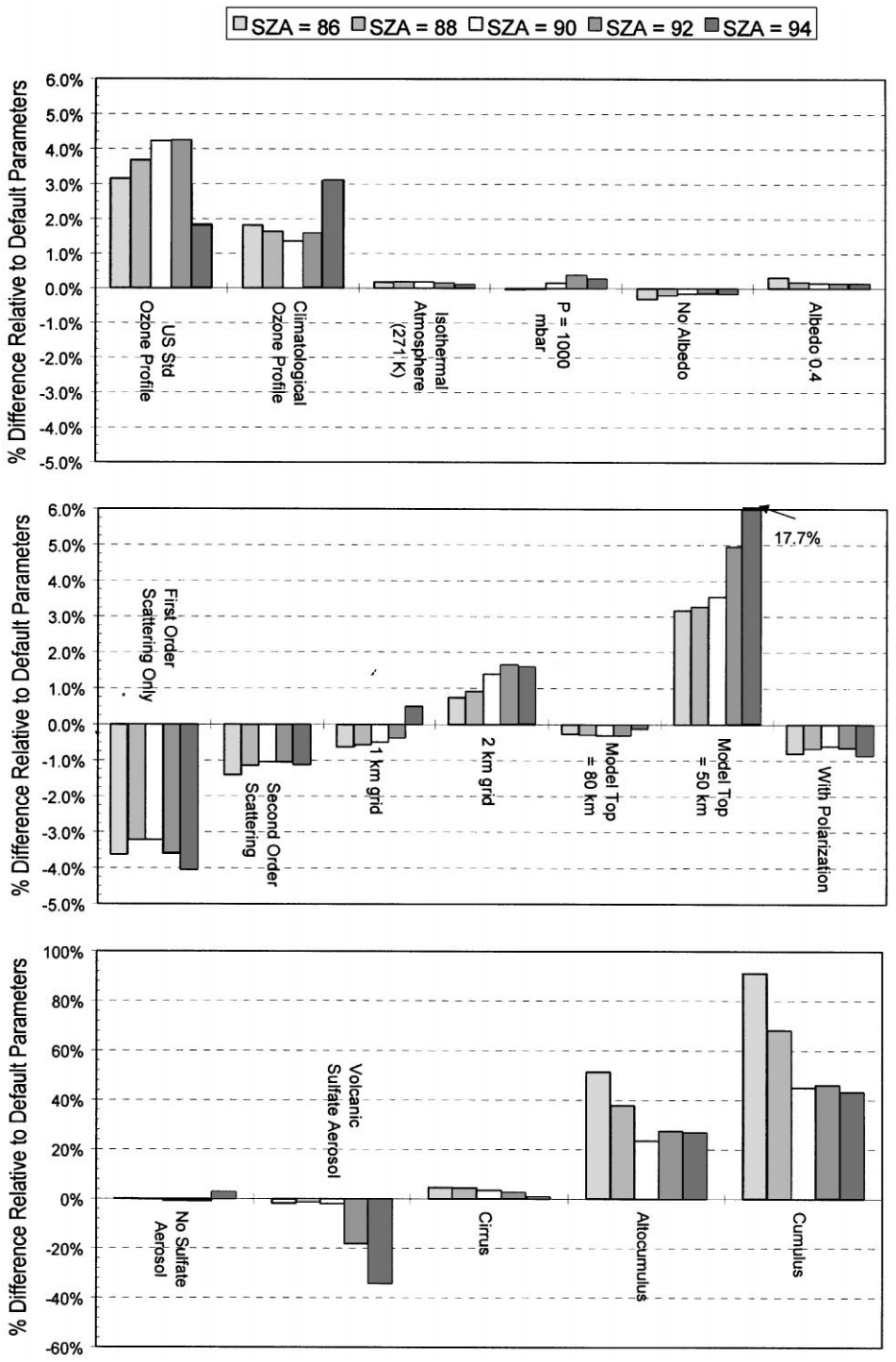

Fig. 3. Variation in ozone AMFs under different RT model parameterizations: (a) geophysical parameters; (b) model parameters; (c) clouds and aerosols.

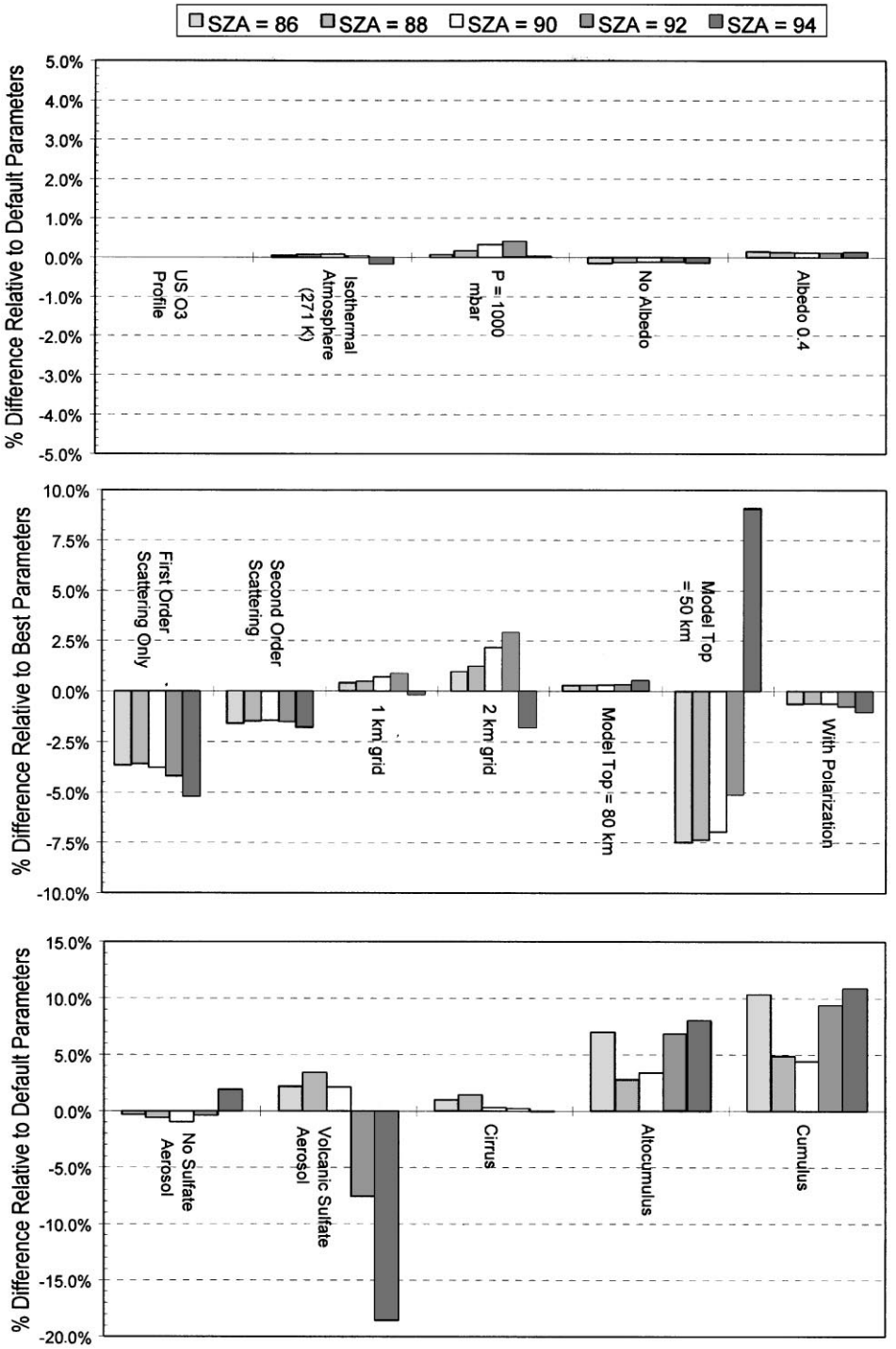

Fig. 4. Variation in NO_2 AMFs under different RT model parameterizations: (a) geophysical parameters; (b) model parameters; (c) clouds and aerosols.

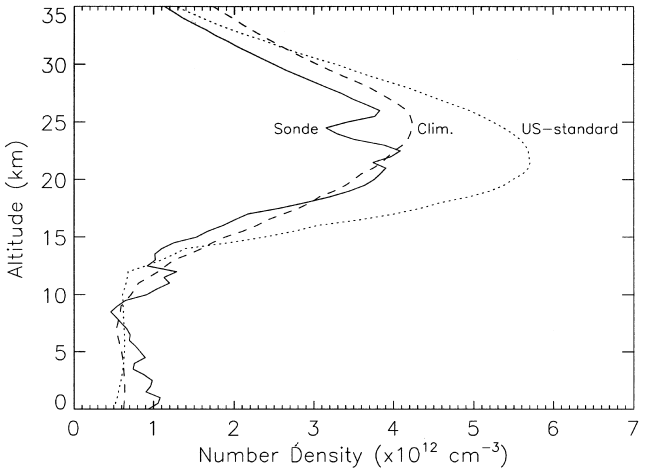

Fig. 5. A comparison of the measured ozone profile with US standard and climatological profiles.

271 K, well away from the temperature at the absorber maximum (220–240 K) was assumed, there were only small changes (less than 0.25%) in AMF. Changing the surface pressure from 955 mbar (observed value) to 1000 mbar also had minimal impact on AMFs.

Increasing the surface albedo from 0.0 to 0.4 had a small, but non-zero effect and although diurnal and seasonal variations in albedo have been observed for mid-latitude arable locations [39] the effect on ozone or NO_2 AMFs is expected to be negligible. The albedo results are slightly different from those of Sarkissian et al. [9] who reported that adding a ground albedo of 0.5 had no effect. However, they also report a small (but unstated) difference in AMF when multiple scattering was included in their model; intuitively, scattered light reflected from the ground back into the atmosphere must be scattered at least once more to reach the zenith-sky spectrometer. It is evident that in RT models, certain parameters can act in tandem with each other (e.g. albedo and multiple scattering) to introduce coupled effects. This is a strong argument for using the most rigorous treatment of the atmosphere that is computationally feasible.

3.2.2. Model parameters

We determined that a single-scattering scheme underestimated AMFs by 3–5% at SZAs between 80 and 95°. Previous studies [9,17] have evaluated second-order scattering models against first-order models and concluded that multiple scattering is important for tropospheric species, but less significant for stratospheric absorbers. Single-scattering models were considered to be a reasonable approximation, and due to limits on computer processing speed, have been commonly used. However, with the recent advances in computer speed, combined with improvements in the accuracy of zenith-sky measurements, it would seem that using an RT model that only considers first-order scattering adds a significant (and unnecessary) error to the AMF calculation.

Turning to consider other computational parameters, a model with a vertical resolution of 1.0 km was found to add little error compared with the default resolution of 0.5 km. There were also only small differences observed when decreasing the atmospheric height from 120 to 80 km.

These are the minimum values we recommend for deriving satisfactory AMFs and are in-line with those suggested by Sarkissan et al. [9]. Significant AMFs changes were observed when the atmospheric height was reduced to 50 km or the resolution degraded to a 2 km grid. As expected, adding polarization to the model had little effect (less than 1%) over all SZAs.

3.2.3. Stratospheric sulfate aerosols

AMFs calculated with no stratospheric sulfate aerosols were only slightly different from those calculated for background aerosol loading. Our AMFs appear to be less sensitive to background aerosols than other studies, which is likely a result of the very low levels of sulfate aerosols currently in the atmosphere. Specifically, the 'background' SAGE II profile used here (from August 1997) is roughly a factor of two smaller through the ozone maximum than the April 1988 used by Sarkissian et al. [9]. Conversely, in a post-volcanic atmosphere such as that following the eruption of Mt. Pinatubo, the extinction coefficient near the absorber can be enhanced by a factor of 20 (see Fig. 2). In this case, stratospheric sulfates were found to exert a strong influence on the calculated AMFs of both ozone and NO_2, particularly at SZAs higher than 90°.

Interestingly, below 90° the effect on ozone and NO_2 AMFs was different; ozone AMFs were decreased at all SZAs of interest whereas for NO_2 a small increase in AMFs was discerned. With increased sulfates present, it would seem that a greater fraction of light collected by the instrument was scattered into its line of sight into or above the bulk of the absorber. Such photons traverse the absorbing layer with an effective AMF of unity and act to decrease the overall AMF. However, why are some of the NO_2 AMFs slightly larger with enhanced aerosols present? To investigate whether these results were due to multiple scattering and increased interstitial absorption in the aerosol layer, the model was re-run with enhanced sulfates but only single-order scattering. In this case, NO_2 AMFs were decreased at all SZAs relative to background aerosol AMFs — very good evidence that multiple scattering becomes even more important to radiative transfer in atmospheres with a high sulfate loading. The difference in the effect on ozone and NO_2 AMFs here is due to their different vertical profiles.

3.2.4. Tropospheric clouds

Of all the factors we investigated, clouds were found to modify AMFs most significantly, implying that if tropospheric clouds are present during zenith-sky observations then default AMFs are unsuitable for calculating vertical column amounts. The results of adding clouds to the RT model are discussed below.

Adding cirrus (Ci) clouds into the model acted to increase AMFs modestly (0–5%), with smaller percentage changes as the SZA increased. This and the behavior of AMFs at smaller SZAs is due to the increase in scattering by the Ci cloud particles. At small SZAs, direct sunlight is scattered downward by the Ci cloud and travels a near-vertical path between cloud and instrument. This acts to decrease the effective AMFs at low SZAs relative to clear-sky AMFs because under clear conditions, direct sunlight traverses the troposphere on a slant path and is zenith-scattered at lower altitudes. However, as SZA increases, the proportion of diffuse skylight to direct sunlight scattered in the zenith by the Ci cloud also increases and the effective AMF is enhanced to the point where the overall Ci AMFs become larger than those for clear skies. At even higher SZAs (over 90°) nearly all direct sunlight is scattered before it even reaches the cloud and the enhancement of Ci AMFs over clear-sky AMFs begins to decrease. An elegant and thorough discussion of this effect is

presented by Pfeilsticker et al. [14]. Other effects of Ci clouds such as interstitial absorption and their tendency to act as a reflective layer of high albedo were found to be minor.

Changes in AMF were more pronounced for model runs containing altocumulus (Ac) or cumulus (Cu) cloud. For both types of cloud, the largest percentage increases in ozone AMFs were at lower SZAs. At a SZA of 90°, adding an Ac cloud to the model increased AMFs by over 20% and for a Cu cloud the increase was in excess of 45%. For NO_2, the pattern was different, with the smallest increase at 90° and larger AMF increases at both lower and higher SZAs. However, the effect of clouds on trace gas AMFs is intimately tied to the vertical profile of that gas and AMFs were recalculated for the Ac cloud, with increased amounts of NO_2 ($3\times$ and $10\times$ more than background concentration) between 0 and 8 km to simulate more urban atmospheres. In the atmospheres with a high tropospheric concentration of NO_2, enhancement factors due to optically thick tropospheric clouds near the surface were found to be quite different to the AMFs calculated assuming background NO_2 concentrations. In both cases, the enhancement in AMF at smaller SZAs was much larger; e.g. AMFs for the $10\times NO_2$ troposphere were enhanced by over 40% at an SZA of 86°. Further, the overall trend was similar to that observed for ozone AMFs; there was a decrease in ΔAMF as SZA increased. This demonstrates that unless tropospheric mixing ratios are accurately known, caution must be exercised when attempting to quantify the effect of tropospheric clouds on zenith-sky light. Mechanisms that modify the geometric path of zenith-scattered light in optically thick clouds are more complex than for the cirrus cloud [15]. Interstitial absorption and photon diffusion in optically thick clouds can lead to largely amplified AMFs, as the calculations presented here suggest.

3.3. The effect of AMFs on retrieved vertical column densities

We next address how changes in AMFs alter the conversion of slant column densities into vertical column densities. Firstly, if Eq. (1) is used to calculate VCDs directly (and a constant value of RCD is assumed) then any percentage change in AMF will alter the denominator and introduce a change of equal proportion in the retrieved VCD. However, if the slope of a Langley plot is used to derive ozone VCDs, this is not necessarily true and the result depends on AMF changes relative to SZA. This can be illustrated by considering the effect of hypothetical AMF changes for the observed ozone SCDs from sunrise on August 20, 1998 (J-232), a period with negligible cloud cover. For example, were there to be a constant AMF shift (e.g. AMF $+1$) across all SZA, the vertical column amount retrieved from the Langley plot would be the same because the slope of the line would be unaffected; rather the intercept would be altered (Fig. 6). Conversely, if all AMFs increased by the same percentage change (e.g. AMF $\times 110\%$), then the Langley intercept would be constant but the gradient would increase accordingly (Fig. 6). In practice, the effect of varying the RT model parameters was found to lie somewhere between the two extremes. Clearly, care must be taken in quantifying potential errors in VCDs derived from Langley analysis simply from AMF differences.

Langley plots for ozone during sunrise on J-232 were constructed for each of the 19 model runs using spectra recorded at SZAs from 80.1 to 93.9°. VCDs and RCDs were calculated from the slope and negative intercept of the linear regression, with the results listed in Table 3. For the atmosphere with a volcanic sulfate loading there was a very poor linear relationship (the regression coefficient was 0.946) between the AMFs and the observed SCDs. There were also large errors introduced due

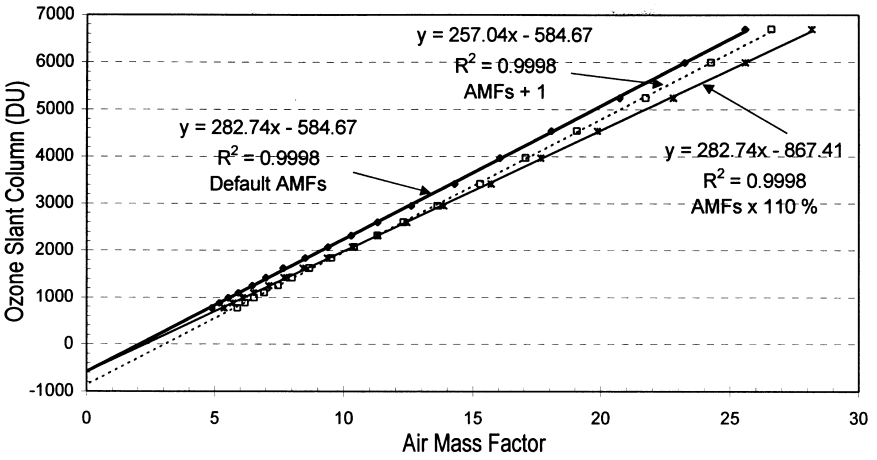

Fig. 6. Langley plots for sunrise on J-232, 1998. The effect of changes in the AMF on slope and y-intercept.

Table 3
Variation in ozone vertical column density as derived from Langley plots

Parameter	Ozone VCD (ΔVCD%)[a]	y-Intercept[b]	Regression coefficient
Default	282.7 (0.0%)	− 584.7	0.9998
US temperature	282.0 (− 0.2%)	− 602.3	0.9997
US O_3 profile	270.9 (− 4.2%)	− 558.5	0.9996
Atmosphere at 241 K	270.7 (− 4.2%)	− 582.4	0.9998
Albedo = 0.0	282.6 (0.0%)	− 574.7	0.9998
Albedo = 0.4	282.8 (0.0%)	− 594.3	0.9998
P = 1000 mbar	281.3 (− 0.5%)	− 573.0	0.9998
With polarization	284.2 (0.5%)	− 576.4	0.9998
Single scattering	292.0 (3.3%)	− 565.6	0.9997
Double scattering	284.7 (0.7%)	− 563.3	0.9998
1 km grid	282.6 (0.0%)	− 567.1	0.9999
2 km grid	277.4 (− 1.9%)	− 558.3	0.9999
Model top = 80 km	283.5 (0.3%)	− 584.8	0.9998
Model top = 50 km	262.2 (− 7.3%)	− 479.1	0.9989
Cirrus at 8 km	279.6 (− 1.1%)	− 676.1	0.9996
Altocumulus: 3–5 km	256.8 (− 9.2%)	− 1503.0	0.9967
Cumulus: 1–5 km	247.9 (− 12.3%)	− 2263.3	0.9961
No aerosol	282.9 (0.1%)	− 581.2	0.9998
Volcanic aerosol	—	—	0.9461

[a]The ΔVCD is relative to the default calculation.
[b]The negative of the y-intercept is representative of the RCD (SCD in the reference spectrum).

to other parameterizations, broadly in agreement with the changes in AMFs themselves (as presented in Fig. 3). Although Langley plots only yield a mean vertical ozone column for a set of twilight spectra, they also provide an effective means to visualize and evaluate the correspondence between AMFs and SCDs. As such these plots present a valuable diagnostic tool in the analysis of

zenith-sky spectra and are essential in determining the effective slant column in the reference spectrum.

4. The influence of clouds on zenith-sky measurements

4.1. Overview

For the majority of the twilight observations made during the MANTRA 1998 campaign, Langley plots revealed a high degree of correlation between ozone SCDs and the default AMFs, with a regression coefficient better than 0.999 in most cases. Furthermore, the y-intercept (negative RCD) for such plots was relatively consistent, with a mean value of -583 DU ($n = 10$, standard deviation ± 18 DU). However, for certain sets of twilight observations, the linear regression between ozone SCD and AMF was poor and/or the value of the RCD was significantly smaller. On such days, semi-quantitative meteorological information revealed the presence of tropospheric clouds. In addition to the effect of clouds on ozone SCDs, the fitted amounts (the apparent optical depths) of NO_2, O_4 and H_2O also increased during overcast conditions. For the transfer of radiation through cloudy skies, the default AMFs did not reproduce the true enhancement factor. Other recent studies [e.g. 13,15,40] have also noted that clouds can influence the observed optical depths of a number of zenith-sky measurements. These studies observed that the fitted amount of O_4 [13,15] or absorption by the O_2 A-band [40] was enhanced in the presence of tropospheric clouds.

Meteorological observations from a station within 25 km of the measurement site and of a very similar elevation (Saskatoon, 52°10′N, 106°41′, elevation 504 m) were obtained from Environment Canada. The observations included cloud opacity, along with height and classification (for each cloud layer), which we used to rudimentarily characterize the sky conditions. AMFs were calculated for three typical cloud scenarios (see Section 3). The effects of two distinct sky conditions on the zenith-sky ozone observations are described below and the feasibility of using revised AMFs to account for tropospheric clouds is discussed.

4.2. Sunset on August 22, 1998 (J-234)

During the MANTRA 1998 campaign, there was one particular day with heavily overcast skies when the effect of tropospheric clouds on the zenith-sky observations was very pronounced, namely the evening of August 22 (J-234). The concurrent meteorological observations are shown in Fig. 7 and reveal a layer of towering cumulus (TCu) cloud with a base height of 1 km and a layer of Ac cloud (base ≈ 3 km) above. The synoptic meteorology at this time was rather dynamic, which resulted in the rapid variation in cloud cover seen in Fig. 7. Fitted amounts of ozone, NO_2,O_4 and H_2O were all substantially enhanced on the evening of J-234 compared with the corresponding amounts for sunset measurements on clear days.

For clear-sky observations, there was a high degree of agreement between the optical depth of O_4 (at 477 nm) and the calculated O_4 AMF at SZAs below 90°, illustrated in Fig. 8. As far as we are aware, the correlation that we discerned is one of the few successful attempts to match O_4 AMFs at 477 nm with zenith-sky observations. The divergence of the clear-sky O_4 measurements with

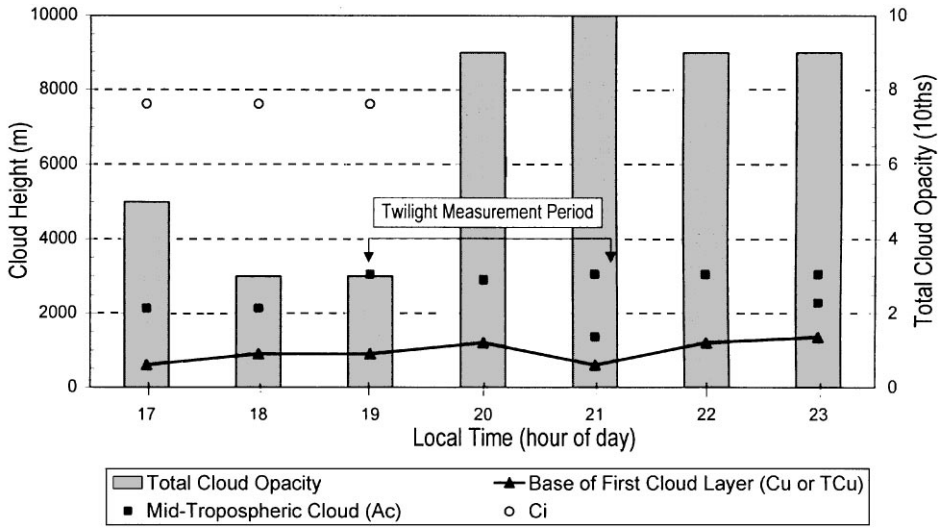

Fig. 7. Cloud base heights and total cloud opacity on J-234, 1998.

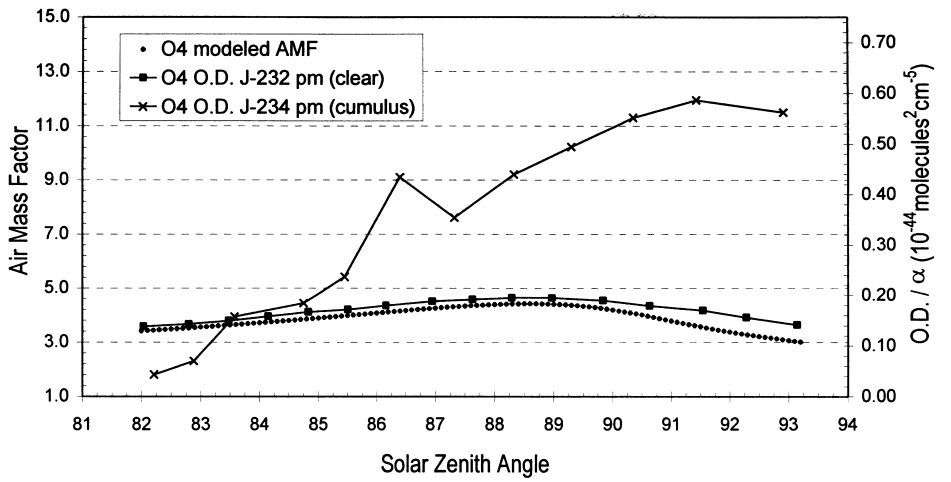

Fig. 8. Observed O_4 SCD and modeled O_4 AMFs for clear sky.

AMFs at SZAs over 90° is probably due to the absence of refraction in our RT model. Refraction can become important for tropospheric absorbers at high SZAs [17]. In contrast to the clear-sky situation, the optical depths of O_4 that we observed during sunset on J-234 were distinctly different. This difference is consistent with the sensitivity of O_4 optical depth to tropospheric clouds. O_4 absorption has been found to increase linearly with AMF (at least up to AMF = 6) [41] and thus is potentially useful for inferring enhanced tropospheric photon pathlengths. However, its profile is strongly altitude dependent and is very sensitive to cloud height. Any uncertainties in the vertical profile of clouds will lead to large errors in the estimated geometric pathlength. For this reason we did not attempt such a calculation.

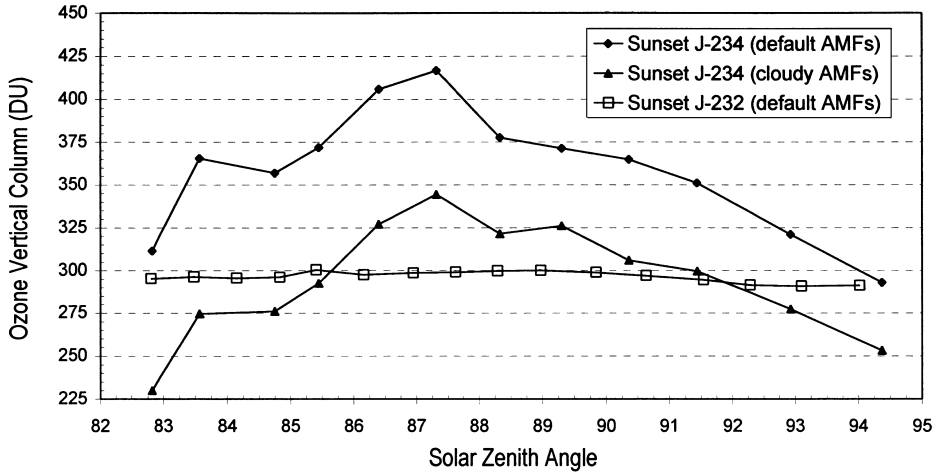

Fig. 9. Comparison of derived ozone VCDs during sunset on J-232 and J-234.

There was no linear correlation between ozone SCDs observed on the evening of J-234 and the default AMFs and consequently Langley plot analysis was precluded. Vertical ozone columns were calculated from Eq. (1) (using RCD derived from clear-sky Langley plots and default AMFs) and are shown in Fig. 9 along with a set of clear-sky sunset VCDs for comparison. It can be seen that the VCDs of ozone were enhanced (by a factor as high as 0.4) and varied by over 100 DU during the cloudy conditions. Following the analysis using default AMFs, revised AMFs were calculated from model runs that included tropospheric clouds at appropriate altitudes and Fig. 9 also contains the VCDs retrieved using the cloudy AMFs. However, while the VCDs were modified and the mean value was more reasonable, they remained highly varied through the measurement period with a poor linear correlation between SCDs and revised AMFs, suggesting that the RT model atmosphere did not reflect the true situation. It is probable (as discussed later) that this is because cloud altitude and optical depth were not sufficiently well characterized.

4.3. Sunrise on August 23, 1998 (J-235)

The cloud cover during sunrise on August 23 (J-235) was characterized by a layer of Ci cloud at an altitude of 8 km. Ac clouds were also observed, but only covering a small proportion of the sky. The deviation of observed SCDs was far less pronounced during measurements under Ci cloud than during the episode of thick tropospheric clouds on J-234 PM, but nevertheless, significant artifacts were present in the data. Interestingly, while the SCDs of NO_2 were visibly enhanced, the fitted amounts of O_4 were quite similar to those observed under clear conditions; an unexpected result that requires further study.

The RCD value derived from the corresponding Langley plot for ozone was only 490 DU compared with the clear-sky mean value of 583 DU. When VCDs were calculated for the sunrise period there was an unusually high degree of variability (between 310.1 and 327.9 DU). Following the analysis of SCD using the default AMFs, VCDs were retrieved using AMFs calculated with a thin layer of Ci cloud (optical depth = 0.1) at 8 km. For the analysis using cirrus AMFs, the

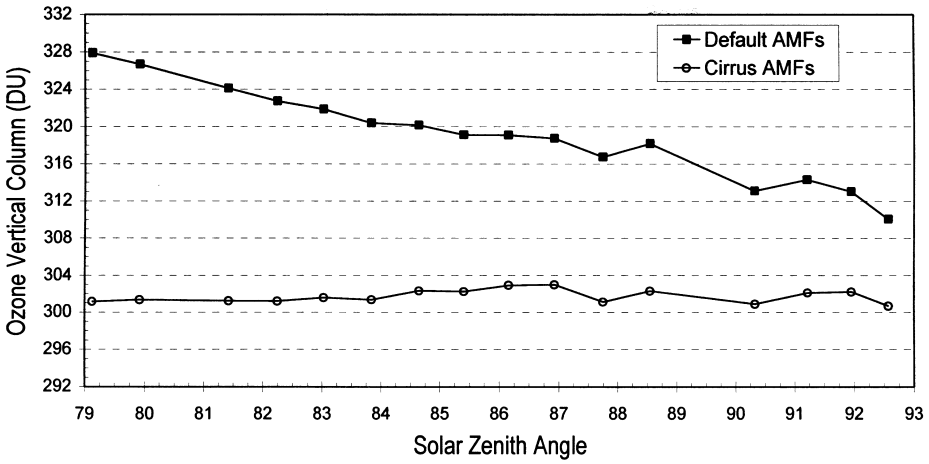

Fig. 10. Comparison of ozone VCDs for sunrise on J-235 using default and modified AMFs.

VCDs were far less variable (300.7–303.0 DU) and more consistent with ozone columns observed on other days during the campaign [19]. Furthermore, the magnitude of the derived RCD was increased to 570 DU which is within one standard deviation of the mean value. The combination of these results suggests that the Ci AMFs we calculated are representative of the modified photon paths induced by the presence of Ci clouds. A comparison between the VCDs retrieved using default AMFs and cirrus AMFs is presented as Fig. 10.

4.4. Discussion

The observations presented in this section illustrate the problems in correcting zenith-sky measurements for the presence of tropospheric clouds but demonstrate that such corrections are possible. In order to model the enhanced AMFs, accurate vertical profiles of the absorber in question and cloud cover information (total opacity of clouds, height of base and top) are necessary. It is also important to know the optical density of the cloud(s) and to identify the number of cloud layers because multiple (so-called 'ping-pong') reflection of photons can occur between cloud layers [14]. In addition to an increase in absorber optical depths due to enhanced photon pathlengths, convection and electrical discharges can amplify the concentrations of ozone and NO_2 present in thunderclouds. Recent measurements of ozone and NO_2 during a thunderstorm [42] suggest that lightning can contribute a substantial amount of 'extra' interstitial NO_2. Intrusion of stratospheric air during thunderstorms can also lead to higher-than-normal tropospheric ozone concentrations. The combined effect of these phenomena is to render accurate zenith-sky measurements under very overcast skies a formidable challenge. Consequently, the diagnosis and characterization of the influence of clouds on UV–visible observations is in its infancy, however, zenith-sky observations present a potentially useful tool for the study of tropospheric cloud processes. Further observational and modeling investigations are merited.

The effect of Ci clouds on zenith-sky measurements is more straightforward than that of optically thick clouds because multiple reflections and the interstitial absorption of photons are

nearly negligible in cirrus. Rather, Ci clouds act to change the contribution of scattered and direct light observed at the ground. The action of these mechanisms on radiative transfer was modeled, and revised AMFs were generated which produced more realistic ozone VCDs and a Langley intercept value consistent with clear-day observations. In summary, if cloud characteristics are well known, and the mechanisms acting to modify absorber optical depths are explicitly understood, then correcting zenith-sky measurements is possible. For less well-defined cases, there are large errors associated with correcting AMFs for the presence of clouds.

5. Conclusions

The sensitivity study that we performed to determine the relative weighting of RT model parameters highlighted that certain inputs exert a strong influence on calculated AMFs, comparable with measurement errors. To reiterate our results:

1. The use of a standard mid-latitude ozone profile was found to introduce relatively large errors (approximately 2.5–5%) in calculated ozone AMFs when compared with the measured profile. These errors were reduced when a climatological profile was used.
2. It was determined that multiple scattering is important in any RT calculation. Perhaps more significant was the influence of multiple scattering on a number of other parameters such as albedo and aerosols. Clearly, multiple scattering should be included in RT models for the purpose of calculating accurate AMFs.
3. A high sulfate aerosol loading was found to modify AMFs substantially, although in an atmosphere with very low background sulfate concentration (such as the late 1990s), sulfate aerosols were found to be relatively insignificant.

In common with other recent studies, our model investigation and zenith-sky observations showed that in the presence of tropospheric clouds, the apparent optical depths of absorbing species can be enhanced. Revised ozone AMFs were applied to two sets of spectra recorded under distinctly different types of cloud cover. For observations taken under a thin Ci cloud, it appears that the revised AMFs successfully modeled the photon path and improved the retrieved VCDs. However, for the more complicated situation also considered, with combined Cu and Ac clouds, it proved impossible to derive a linear relationship between AMFs and SCDs. Further investigation into the effect of clouds on zenith-sky measurements is timely and could prove to be valuable in arriving at a better understanding of cloud processes.

Acknowledgements

M.R.B. was supported by funding from the Canadian Space Agency (CSA) and the Natural Sciences and Engineering Research Council of Canada (NSERC). The zenith-sky instrument was also funded by NSERC. The MANTRA field campaign was supported by the CSA, Environment Canada, and the Centre for Research in Earth and Space Technology (CRESTech). The authors are grateful to Tom Mathews and Clive Midwinter of Environment Canada for providing the meteorological information and especially Colette Heald for her help in analyzing the cloud data.

References

[1] Noxon JF, Whipple Jr. EC, Hyde RS. Stratospheric NO_2, 1, observational method and behavior at mid-latitude. J Geophys Res 1979;84:5047–66.
[2] Solomon S, Sanders RW, Carroll MA, Schmeltekopf AL. Visible and near-ultraviolet spectroscopy at McMurdo station, Antarctica 5. Observations of the diurnal variations of BrO and OClO. J Geophys Res 1989;94: 11,393–403.
[3] Fish DJ, Jones RL, Strong EK. Midlatitude observations of the diurnal variation of stratospheric BrO. J Geophys Res 1995;100:18,863–71.
[4] Otten C, Ferlemann F, Platt U, Wagner T, Pfeilsticker K. Ground-based DOAS UV/visible measurements at Kiruna (Sweden) during the SESAME winters 1993/94 and 1994/95. J Atmos Chem 1998;30:141–62.
[5] McElroy CT, McLinden CA, McConnell JC. Evidence of bromine monoxide in the free troposphere during the Arctic polar sunrise. Nature 1999;397:338–41.
[6] Burrows JP, Weber M, Buchwitz M, Rozanov V, Ladstatter-Weissenmayer A, Richter A, DeBeek R, Hoogen R, Bramstedt K, Eichmann KU, Eisinger M. The global ozone monitoring experiment (GOME): mission concept and first scientific results. J Atmos Sci 1999;56:127–50.
[7] Solomon S, Schmeltekopf AL, Saunders RW. On the interpretation of zenith-sky absorption measurements. J Geophys Res 1987;92:8311–9.
[8] Platt U. Differential optical absorption spectroscopy (DOAS). In: Sigrist MW, editor. Air monitoring by spectroscopic techniques. Chemical Analysis Series, vol. 127. New York: Wiley, 1994.
[9] Sarkissian A, Roscoe HK, Fish DJ. Ozone measurements by zenith-sky spectrometers: an evaluation of errors in air-mass factors calculated by radiative transfer models. JQSRT 1995;54:471–80.
[10] Slusser J, Hammond K, Kylling A, Stamnes K, Perliski L, Dahlback A, Anderson D, DeMajistre R. Comparison of air mass computations. J Geophys Res 1996;101:9315–21.
[11] U.S. Standard Atmosphere. National Oceanic and Atmospheric Adminstration, National Aeronautics and Space Administration, and United States Air Force, Washington, DC, 1976.
[12] Valley SL. Handbook of geophysics and space environments. New York: McGraw-Hill, 1965.
[13] Erle F, Pfeilsticker K, Platt U. On the influence of tropospheric clouds on zenith-scattered-light measurements of stratospheric species. Geophys Res Lett 1995;22:2725–8.
[14] Pfeilsticker K, Erle F, Funk O, Marquard L, Wagner T, Platt U. Optical path modifications due to tropospheric clouds: implications for zenith sky measurements of stratospheric gases. J Geophys Res 1998;103:25, 323–35.
[15] Pfeilsticker K, Arlander DW, Burrows JP, Erle F, Gil M, Goutail F, Hermans C, Lambert JC, Platt U, Pommereau JP, Richter A, Sarkissian A, Van Roozendael M, Wagner T, Winterrath T. Intercomparison of the influence of tropospheric clouds on UV-visible absorptions detected during the NDSC intercomparison campaign at OHP in June 1996. Geophys Res Lett 1999;26:1169–72.
[16] Wagner T, Erle F, Marquard L, Otten C, Pfeilsticker K, Senne T, Stutz J, Platt U. Cloudy sky optical paths as derived from differential optical absorption spectroscopy observations. J Geophys Res 1998;103:25, 307–21.
[17] Perliski LM, Solomon S. On the evaluation of air mass factors for atmospheric near ultra-violet and visible absorption spectroscopy. J Geophys Res 1993;98:10,363–74.
[18] Strong K, Bailak G, Barton D, Bassford MR, Blatherwick RD, Brown S, Chartrand D, Davies J, Drummond JR, Fogal PF, Forsberg E, Hall R, Jofre A, Kaminski J, Kosters J, Laurin C, McConnell JC, McElory CT, Menzies K, Midwinter C, Murcray FJ, Olson RJ, Quine BM, Rochon Y, Savastiouk V, Solheim B, Sommerfeldt D, Ullberg A, Werchohlad S, Wunch D. MANTRA — a balloon mission to study the odd-nitrogen budget of the stratosphere. Atmos Ocean, in preparation.
[19] Bassford MR, Strong K, McLinden CA, Davies J, Savastiouk V. Ground-based measurements of ozone and NO_2 during MANTRA 1998 using a new zenith-sky spectrometer. Atmos Ocean 2000, submitted for publication.
[20] Roscoe HK, Fish DJ, Jones RL. Interpolation errors in UV–visible spectroscopy for stratospheric sensing; implications for sensitivity spectral resolution and spectral range. Appl Opt 1996;35:427–32.
[21] Roscoe HK, Johnston PV, Van Roozendael M, Richter A, Sarkissian A, Roscoe J, Preston KE, Lambert JC, Hermans C, Decuyper W, Dzienus S, Winterrath T, Burrows J, Goutail F, Pommereau JP, D'Almeida E, Hottier J, Coureul C, Didier R, Pundt I, Bartlett LM, McElroy CT, Kerr JE, Elokhov A, Giovanelli G, Ravegnani F,

Premuda M, Kostadinov I, Erle F, Wagner T, Pfeilsticker K, Kenntner M, Marquard LC, Gil M, Puentedura O, Yela M, Arlander DW, Hoiskar BAK, Tellefsen CW, Tornkvist KK, Heese B, Jones RL, Aliwell SR, Freshwater RA. Slant column measurements of O_3 and NO_2 during the NDSC intercomparison of zenith-sky UB–visible spectrometers in June 1996. J Atmos Chem 1999;32:281–314.

[22] Koike M, Kondo Y, Matthews WA, Johnston PV, Nakajima H, Kawaguchi A, Nakane H, Murata I, Budiyono A, Kanada M, Toriyama N. Assessment of the uncertainties in the NO_2 and O_3 measurements by visible spectrometers. J Atmos Chem 1999;32:121–45.

[23] Burrows JP, Richter A, Dern A, Deters B, Himmelmann S, Voight S, Orphal J. Atmospheric remote-sensing reference data from GOME. Part 2: temperature-dependent absorption cross-sections of O_3 in the 231–794 nm range. JQSRT 1999;61:509–17.

[24] Burrows JP, Dern A, Deters B, Himmelmann S, Richter A, Voight S, Orphal J. Atmospheric remote-sensing reference data from GOME. Part 1: temperature-dependent absorption cross-sections of NO_2 in the 231–794 nm range. JQSRT 1998;60:1025–31.

[25] Sarkissian A. PhD thesis, Université de Paris 6, 1992.

[26] Greenblatt GD, Orlando JJ, Burkholder JB, Ravishankara AR. Absorption measurements of oxygen between 330 and 1140 nm. J Geophys Res 1990;95:18,577–82.

[27] Chance KV, Spurr RJD. Ring effect studies: Rayleigh scattering, including molecular parameters for rotational Raman scattering, and the Fraunhofer spectrum. Appl Opt 1997;36:5224–30.

[28] Roscoe HK, Squires AC, Oldham DJ, Sarkissian A, Pommereau J-P, Goutail F. Improvements to the accuracy of zenith-sky measurements of total ozone by visible spectrometers. JQSRT 1994;52:639–48.

[29] Vaughan G, Roscoe HK, Bartlett LM, O'Connor FM, Sarkissian A, Van Roozendael M, Lambert JC, Simon PC, Karlsen K, Hoiskar BAK, Fish DJ, Jones RL, Freshwater RA, Pommereau JP, Goutail F, Andersen SB, Drew DG, Hughes PA, Moore D, Mellqvist J, Hegels E, Klupfel T, Erle F, Pfeilsticker K, Platt U. An intercomparison of ground-based UV–visible sensors of ozone and NO_2. J Geophys Res 1997;102:1411–22.

[30] Lee AM, Roscoe HK, Oldham DJ, Squires AC, Sarkissian A, Pommereau J-P, Gardiner BG. Improvements to the accuracy of measurements of NO_2 by zenith-sky visible spectrometers. JQSRT 1994;52:649–57.

[31] McLinden CA. Observation of atmospheric composition from NASA ER-2 spectroradiometer measurements. PhD thesis, York University, Toronto, Canada, 1998. p. 292.

[32] McLinden CA, McConnell JC, Griffioen E, McElroy CT. A vector radiative transfer model for the Odin/OSIRIS project. Can J Phys 2000, accepted for publication.

[33] Hansen JE, Travis LD. Light scattering in planetary atmospheres. Space Sci Rev 1974;16:527–610.

[34] Evans KF, Stephens GL. A new polarized atmospheric radiative transfer model. JQSRT 1991;46:413–23.

[35] Stammes P, de Haan JF, Hovenier JW. The polarized internal radiation field of a planetary atmosphere. Astron Astrophys 1989;225:239–59.

[36] Thomason LW, Poole LR, Deshler T. A global climatology of stratospheric aerosol surface area density deduced from Stratospheric Aerosol and Gas Experiment II measurements: 1984–1994. J Geophys Res 1997;102:8967–76.

[37] Betts AK, Ball JH. Albedo over the boreal forest. J Geophys Res 1997;102:28,901–9.

[38] Remsberg EE, Prather MJ. The atmospheric effects of stratospheric aircraft: report of the 1992 models and measurements workshop. NASA Ref. Publ. 1292, 1993.

[39] Song J. Phenological influences on the albedo of prairie grassland and crop fields. Int J Biometeorol 1999;42:153–7.

[40] Min Q, Harrison L. Joint statistics of photon pathlength and cloud optical depth. Geophys Res Lett 1999;26:1425–8.

[41] Michalsky J, Beuaharnois M, Berndt J, Harrison P, Kiedron P, Min Q. O_2–O_2 absorption band identification based on optical depth spectra of the visible and near-infrared. Geophys Res Lett 1999;26:1581–4.

[42] Winterrath T, Kurosu TP, Richter A, Burrows JP. Enhanced O_3 and NO_2 in thunderstorm clouds: convection or production?. Geophys Res Lett 1999;26:1291–4.